

# Compact grating coupler array for multicore fiber fabricated with DUV lithography

Lucas G. Rocha

*School of Electrical and Computer Engineering  
University of Campinas  
Campinas, Brazil  
1172766@unicamp.br*

Julian L. Pita Ruiz

*School of Electrical and Computer Engineering  
University of Campinas  
Campinas, Brazil  
jpita@unicamp.br*

Lucas H. Gabrielli

*School of Electrical and Computer Engineering  
University of Campinas  
Campinas, Brazil  
lhg28@unicamp.br*

**Abstract**—Using Space-Division Multiplexing (SDM) through multicore optical fibers (MCFs) can significantly increase the transmission capacity. However, compatibility with silicon photonics, a promising technology for compact, low-cost and power-efficient devices, requires integration between the two platforms. Using uniform grating couplers combined with compact tapers, two arrays—for  $0^\circ$  and  $10^\circ$ —were designed, fabricated and experimentally characterized. Simulations indicate coupling efficiencies of  $-4.64$  dB and  $-3.64$  dB for the  $0^\circ$  and  $10^\circ$  couplers, respectively, with bandwidths of  $66.5$  nm and  $127.3$  nm. Experimental results yielded efficiencies of  $-6.8$  dB for both designs, and corresponding bandwidths of  $46.8$  nm and  $90$  nm.

**Index Terms**—Multicore fiber, Silicon photonics, Grating coupler

## I. INTRODUCTION

Exploring SDM by means of MCFs can increase the transmission capacity of a single fiber by exploiting its spatial dimension. Due to its multiplexing characteristics, this type of fiber rises as a strong alternative to overcome the incoming transmission capacity crunch [1]–[7] and to improve the performance of data center networks [8]–[10]. Meanwhile, silicon photonics can provide a compact, low-cost, energy saving, high speed, and high density platform [11]–[18], suitable for next-generation optical communications devices. Hence, the interconnection between silicon photonics and MCFs has a fundamental role in enabling both technologies to support future, high data rate optical networks.

Surface coupling via a grating coupler array is the most practical mean to couple a signal from a conventional triangular lattice MCF to integrated silicon waveguides, since edge coupling cannot access all cores. Although there have been a few reported couplers for MCFs, they involve additional

This study was financed in part by the Coordenação de Aperfeiçoamento de Pessoal de Nível Superior - Brasil (CAPES) - Finance Code 88881.311020/2018; FAPESP proc. 2019/01771-7, 2015/24517-8, 2016/19270-6, and 2018/25339-4; CNPq proc. 302036/2018-0.

978-0-7381-2418-6/21/\$31.00 ©2021 IEEE

fabrication steps, such as using a metallic mirror below the substrate [19] or a poly-silicon overlay [20]. Some works use adiabatic tapers [19], [21] that consume a large space on the chip. Focusing grating couplers can reduce the footprint area, enabling a grating array for a 37-core MCF coupler [22]. However, even when using focusing grating couplers, the lowest separation distance between cores that can be coupled into a chip is around  $40\mu\text{m}$ . Our group recently reported low-loss arrays, fabricated on electron beam lithography, for single and dual-polarization MCF-coupling, using state-of-the-art optimization methods [23].

This work reports on two Complementary Metal-Oxide-Semiconductor (CMOS)-compatible, compact grating coupler arrays to couple a  $35\mu\text{m}$  core-separation MCF, as illustrated in Fig. 1. Straight uniform grating couplers for vertical and  $10^\circ$  coupling were designed and simulated using two-dimensional Finite-Difference Time-Domain (FDTD) method. The obtained structures were combined with an optimized  $10\mu\text{m} \times 10\mu\text{m}$  taper and simulated using three-dimensional FDTD. The resulting structures were fabricated through Deep Ultraviolet (DUV) lithography at an external foundry, enabling large-volume production. The fabricated devices were experimentally characterized.

## II. DEVICE DESIGN

Grating couplers are periodic structures used to change the propagation direction of light from a waveguide to a fiber and vice-versa. The simplest structure for this device uses a uniform period, which is obtained through the phase-matching equation [24]–[26], from which two gratings were designed to operate on a wavelength of  $1550$  nm, for fiber tilt angles of  $0^\circ$  and  $10^\circ$ , with periods of  $576.32$  nm and  $625.66$  nm, respectively. They were simulated in two dimensional FDTD for maximization of the coupling efficiency with respect to the grating period, fill factor and corrosion depth allowed in the fabrication.

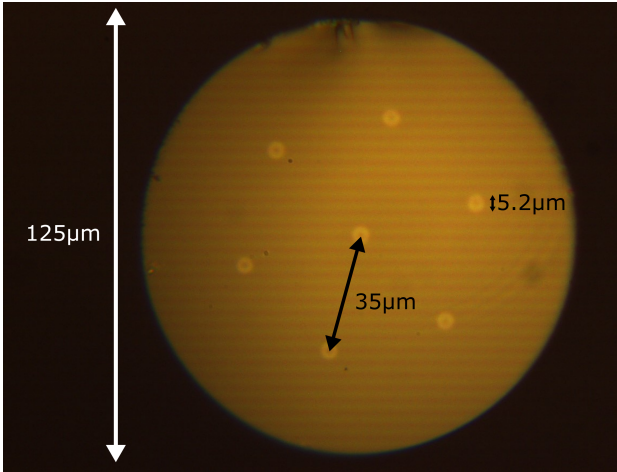


Fig. 1: Optical microscopy image of the cross-section of the MCF, indicating the core diameter, separation distance between adjacent cores and cladding diameter.

Focusing grating couplers are generally used to couple light from a conventional single mode fiber (SMF) to an integrated silicon waveguide, since they provide compactness without efficiency penalty [26], [27]. Earlier, a coupler composed by a long adiabatic taper combined with a straight grating was largely used for the same purpose [25], [28]. However, both approaches are incompatible with MCF coupling with core separation lower than  $40\ \mu\text{m}$ , because there is not enough room to layout the waveguide network connecting to all gratings. To overcome this issue, we designed a compact taper using a topological derivative optimization method [29], which, in combination with a straight grating, reduces the footprint area of the coupler. The dimensions of the taper are  $10\ \mu\text{m} \times 10\ \mu\text{m}$ , enabling low-core separation MCF coupling to silicon photonics. Figure 2(a) shows the three dimensional simulated coupling efficiency of the optimized taper, and Fig. 2(b) shows an illustration of its geometry.

The parameters of the gratings obtained in the two dimensional simulations were combined with the compact taper and simulated using three dimensional FDTD. Figure 3 shows the simulation results of the two resulting devices.

For the  $0^\circ$  grating, the maximum simulated coupling efficiency is  $-4.64\ \text{dB}$  at  $1566.5\ \text{nm}$ , with a  $-3\ \text{dB}$  bandwidth of  $66.5\ \text{nm}$ . A second operation window with  $64\ \text{nm}$  can also be seen in Fig. 3 with a maximum of  $-5.57\ \text{dB}$  at  $1592.18\ \text{nm}$  wavelength. The two windows are separated by a low efficiency valley at  $1579.8\ \text{nm}$  that corresponds to the well-known second diffraction order of the grating backscattering into the feed waveguide [17], [30]–[32]. The  $10^\circ$  coupler optimization yielded a maximum simulated coupling efficiency of  $-3.64\ \text{dB}$  at  $1556.52\ \text{nm}$ , with a  $-3\ \text{dB}$  bandwidth of  $127.3\ \text{nm}$ .

The grating couplers were arranged in a triangular lattice separated by  $35\ \mu\text{m}$ , to match the MCF core distance, and were fed by seven single-mode waveguides coupled to conventional focusing grating couplers. The device was fabricated in a multi-project wafer (MPW) run at Interuniversity Microelec-

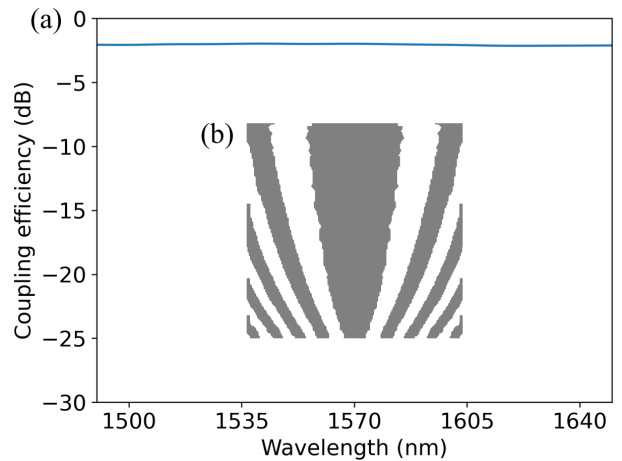


Fig. 2: (a) Coupling efficiency of the compacted taper obtained by three dimensional FDTD simulation. The taper presented a coupling efficiency around  $-2\ \text{dB}$  on the entire simulated band. (b) Geometry of the compact taper obtained on the topological derivative optimization process.

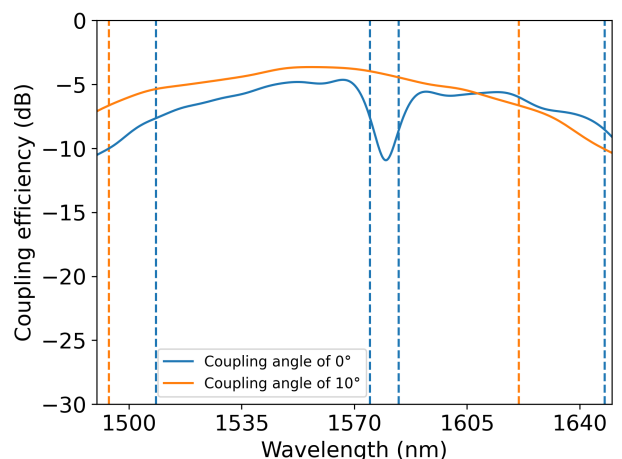


Fig. 3: Simulated coupling efficiency of the couplers obtained by a combination of straight teeth gratings and the compact taper, for coupling angles of  $0^\circ$  and  $10^\circ$ . The dashed lines indicate the  $-3\ \text{dB}$  bandwidth.

tronics Center (IMEC). Figure 4 shows a microscope picture of the fabricated device and a highlight of the grating coupler array, where the compact tapers can be seen in more detail.

### III. EXPERIMENTAL RESULTS

The fabricated devices were experimentally characterized using a tunable laser source (TLS) feeding a conventional SMF, that passes on a polarization controller and is coupled into the device on the feeding waveguides. The output signal is launched into the MCF connected to a power meter. The setup illustrated by Fig. 5(a). To measure the inter-core crosstalk, a conventional single-core SMF is positioned on a 3-axis stage, butt-coupled to the MCF and connected to an optical spectrum analyzer (OSA), as illustrated in Fig. 5(b).

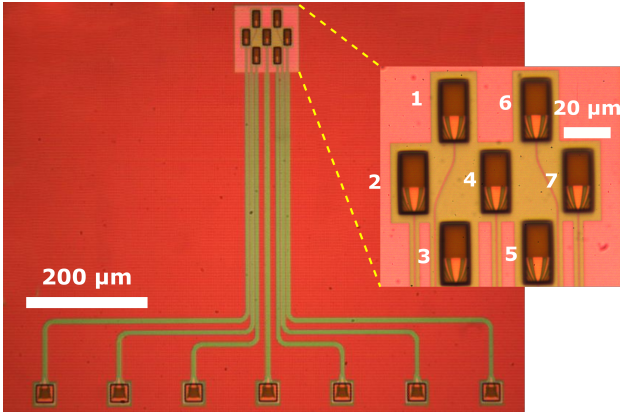


Fig. 4: Optical microscopy image of one of the fabricated MCF couplers, showing the compact coupler array connected to individual conventional focusing grating couplers that were used as input in this experiment. The zoomed area corresponds to the array of couplers to match the MCF cores.

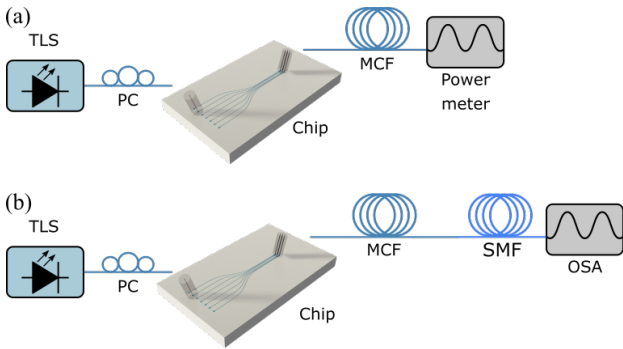
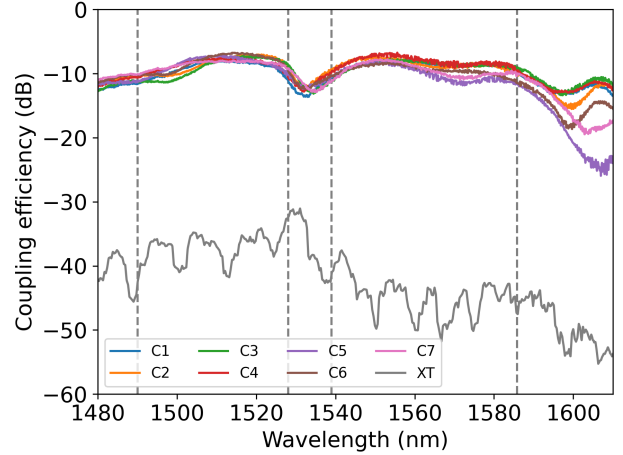


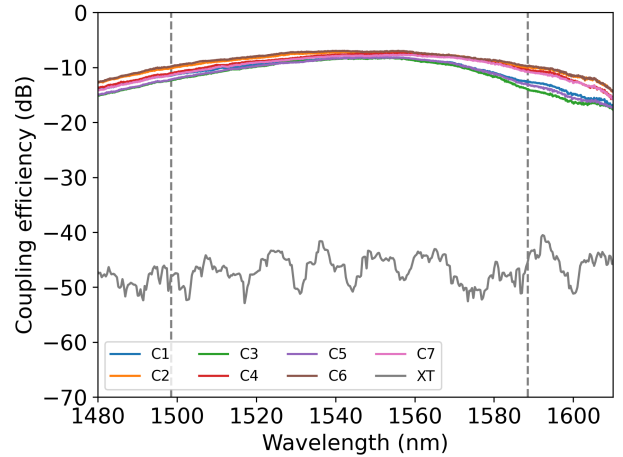
Fig. 5: Illustration of the experimental setups used to measure the (a) coupling efficiency and (b) inter-core cross-talk of the fabricated devices.

The experimental results obtained for the insertion loss of each grating in the array for both devices are shown in Fig. 6. The  $0^\circ$  coupler presented a peak coupling efficiency, for the central core (C4), of  $-6.8$  dB at  $1553.7$  nm, corresponding to a  $-3$  dB bandwidth of  $46.8$  nm and an inter-core cross-talk lower than  $-30$  dB. A second operation window can be seen, with a peak coupling efficiency of  $-7.6$  dB at  $1511.3$  nm and bandwidth of  $38$  nm. The coupler presents the efficiency valley caused by the back reflection of the second-order diffraction, as seen in the simulation, although at  $1532$  nm. The central wavelength of this valley diverges from the simulation mostly due to fabrication variations in the grating. Due to the absence of index-matching fluid, the coupling efficiency varies between different cores, with maximum differences of  $3.8$  dB and  $4.2$  dB at the operating band for the  $0^\circ$  and  $10^\circ$  couplers, respectively. For the  $10^\circ$  grating array, the peak coupling efficiency is  $-6.8$  dB at  $1542.3$  nm, corresponding to a  $-3$  dB bandwidth of  $90$  nm—significantly larger than the usual  $60$  nm bandwidth of conventional grating couplers—for the nearest core to the chip surface. The coupler presented

an inter-core cross-talk lower than  $-40$  dB. The coupling efficiency is approximately  $2.5$  dB lower than the simulated, as a result of fabrication imperfections and the absence of an index-matching fluid, which is included in the simulations.



(a)



(b)

Fig. 6: Measured coupling efficiency of the fabricated couplers for each coupler of the array matching a single core of the fiber, as indicated in Fig. 4, for a coupling angle of (a)  $0^\circ$ ; (b)  $10^\circ$ . The gray lines in both figures correspond to the measured inter-core crosstalk between the central core and a random adjacent outer core. The dashed lines indicate the  $-3$  dB bandwidth

#### IV. CONCLUSIONS

This paper presents compact couplers for  $0^\circ$  and  $10^\circ$  coupling between MCFs and Silicon Photonics, with peak coupling efficiencies of  $-6.8$  dB at  $1553.7$  nm and  $1542.3$  nm, operation bandwidths of  $46.8$  nm and  $90$  nm, and inter-core cross-talks lower than  $-30$  dB and  $-40$  dB, respectively. These are the first results of fiber-to-chip coupling in a MCF with core spaced as close as  $35$   $\mu\text{m}$ , fabricated in a commercial

foundry, and demonstrate the possibility of integrating MCFs in SDM systems with conventional silicon photonics.

## REFERENCES

- [1] E. B. Desurvire, "Capacity Demand and Technology Challenges for Lightwave Systems in the Next Two Decades," *Journal of Lightwave Technology*, vol. 24, pp. 4697–4710, Dec. 2006.
- [2] R.-J. Essiambre and R. W. Tkach, "Capacity Trends and Limits of Optical Communication Networks," *Proceedings of the IEEE*, vol. 100, pp. 1035–1055, May 2012.
- [3] P. J. Winzer, D. T. Neilson, and A. R. Chraplyvy, "Fiber-optic transmission and networking: the previous 20 and the next 20 years [Invited]," *Optics Express*, vol. 26, p. 24190, Sept. 2018.
- [4] P. J. Winzer and D. T. Neilson, "From Scaling Disparities to Integrated Parallelism: A Decathlon for a Decade," *Journal of Lightwave Technology*, vol. 35, pp. 1099–1115, Mar. 2017.
- [5] Y. Awaji, J. Sakaguchi, B. J. Puttnam, R. S. Luís, J. M. D. Mendinueta, W. Klaus, and N. Wada, "High-capacity transmission over multi-core fibers," *Optical Fiber Technology*, vol. 35, pp. 100–107, Feb. 2017.
- [6] K. Saitoh and S. Matsuo, "Multicore Fiber Technology," *Journal of Lightwave Technology*, vol. 34, pp. 55–66, Jan. 2016.
- [7] D. J. Richardson, J. M. Fini, and L. E. Nelson, "Space-division multiplexing in optical fibres," *Nature Photonics*, vol. 7, pp. 354–362, May 2013.
- [8] Y. Liu, H. Yuan, A. Peters, and G. Zervas, "Comparison of SDM and WDM on Direct and Indirect Optical Data Center Networks," p. 3.
- [9] L. Zhang, J. Chen, E. Agrell, R. Lin, and L. Wosinska, "Enabling Technologies for Optical Data Center Networks: Spatial Division Multiplexing," *Journal of Lightwave Technology*, vol. 38, pp. 18–30, Jan. 2020.
- [10] H. Yuan, M. Furdek, A. Muhammad, A. Saljoghei, L. Wosinska, and G. Zervas, "Space-Division Multiplexing in Data Center Networks: On Multi-Core Fiber Solutions and Crosstalk-Suppressed Resource Allocation," *Journal of Optical Communications and Networking*, vol. 10, p. 272, Apr. 2018.
- [11] A. Biberman, S. Manipatrani, N. Ophir, L. Chen, M. Lipson, and K. Bergman, "First demonstration of long-haul transmission using silicon microring modulators," *Optics Express*, vol. 18, p. 15544, July 2010.
- [12] M. Lipson, "Guiding, modulating, and emitting light on Silicon-challenges and opportunities," *Journal of Lightwave Technology*, vol. 23, pp. 4222–4238, Dec. 2005.
- [13] A. Rahim, T. Spuesens, R. Baets, and W. Bogaerts, "Open-Access Silicon Photonics: Current Status and Emerging Initiatives," *Proceedings of the IEEE*, vol. 106, pp. 2313–2330, Dec. 2018.
- [14] D. Thomson, A. Zilkie, J. E. Bowers, T. Komljenovic, G. T. Reed, L. Vivien, D. Marris-Morini, E. Cassan, L. Viot, J.-M. Fédéli, J.-M. Hartmann, J. H. Schmid, D.-X. Xu, F. Boeuf, P. O'Brien, G. Z. Mashanovich, and M. Nedeljkovic, "Roadmap on silicon photonics," *Journal of Optics*, vol. 18, p. 073003, July 2016.
- [15] W. Shi, Y. Tian, and A. Gervais, "Scaling capacity of fiber-optic transmission systems via silicon photonics," *Nanophotonics*, vol. 9, pp. 4629–4663, Nov. 2020.
- [16] P. Dong, Y.-K. Chen, G.-H. Duan, and D. T. Neilson, "Silicon photonic devices and integrated circuits," *Nanophotonics*, vol. 3, pp. 215–228, Aug. 2014.
- [17] L. Chrostowski and M. Hochberg, *Silicon Photonics Design*. Cambridge: Cambridge University Press, 2015.
- [18] X. Chen, M. M. Milosevic, S. Stankovic, S. Reynolds, T. D. Bucio, K. Li, D. J. Thomson, F. Gardes, and G. T. Reed, "The Emergence of Silicon Photonics as a Flexible Technology Platform," *Proceedings of the IEEE*, vol. 106, pp. 2101–2116, Dec. 2018.
- [19] Y. Ding, F. Ye, C. Peucheret, H. Ou, Y. Miyamoto, and T. Morioka, "On-chip grating coupler array on the SOI platform for fan-in/fan-out of MCFs with low insertion loss and crosstalk," *Optics Express*, vol. 23, p. 3292, Feb. 2015.
- [20] Y. Tong, W. Zhou, and H. K. Tsang, "Efficient perfectly vertical grating coupler for multi-core fibers fabricated with 193 nm DUV lithography," *Optics Letters*, vol. 43, p. 5709, Dec. 2018.
- [21] C. R. Doerr and T. F. Taunay, "Silicon Photonics Core-, Wavelength-, and Polarization-Diversity Receiver," *IEEE Photonics Technology Letters*, vol. 23, pp. 597–599, May 2011.
- [22] V. I. Kopp, J. Park, M. Wlodawski, E. Hubner, J. Singer, D. Neugroschl, A. Z. Genack, P. Dumon, J. Van Campenhout, and P. Absil, "Two-Dimensional, 37-Channel, High-Bandwidth, Ultra-Dense Silicon Photonics Optical Interface," *Journal of Lightwave Technology*, vol. 33, pp. 653–656, Feb. 2015.
- [23] J. L. P. Ruiz, L. G. Rocha, J. Yang, S. E. Kocabas, M.-J. Li, I. Aldaya, P. Dainese, and L. H. Gabrielli, "Compact Dual-Polarization Silicon Integrated Couplers for Multicore Fibers," *arXiv:2102.08918 [physics]*, Feb. 2021. arXiv: 2102.08918.
- [24] Y. Wang, J. Flueckiger, C. Lin, and L. Chrostowski, "Universal grating coupler design," (Ottawa, Canada), p. 89150Y, Oct. 2013.
- [25] D. Taillaert, P. Bienstman, and R. Baets, "Compact efficient broadband grating coupler for silicon-on-insulator waveguides," *Optics Letters*, vol. 29, p. 2749, Dec. 2004.
- [26] A. Mekis, S. Gloeckner, G. Masini, A. Narasimha, T. Pinguet, S. Sahni, and P. De Dobbelaere, "A Grating-Coupler-Enabled CMOS Photonics Platform," *IEEE Journal of Selected Topics in Quantum Electronics*, vol. 17, pp. 597–608, May 2011.
- [27] F. Van Laere, T. Claes, J. Schrauwen, S. Scheerlinck, W. Bogaerts, and P. De Dobbelaere, "A Grating-Coupler-Enabled CMOS Photonics Platform," *IEEE Photonics Technology Letters*, vol. 19, pp. 1919–1921, Dec. 2007.
- [28] Y. Fu, T. Ye, W. Tang, and T. Chu, "Efficient adiabatic silicon-on-insulator waveguide taper," *Photonics Research*, vol. 2, p. A41, June 2014.
- [29] J. L. Pita Ruiz, A. A. S. Amad, L. H. Gabrielli, and A. A. Novotny, "Optimization of the electromagnetic scattering problem based on the topological derivative method," *Optics Express*, vol. 27, p. 33586, Nov. 2019.
- [30] Xia Chen, Chao Li, and Hon Ki Tsang, "Fabrication-Tolerant Waveguide Chirped Grating Coupler for Coupling to a Perfectly Vertical Optical Fiber," *IEEE Photonics Technology Letters*, vol. 20, pp. 1914–1916, Dec. 2008.
- [31] Bin Wang, Jianhua Jiang, and G. Nordin, "Embedded slanted grating for vertical coupling between fibers and silicon-on-insulator planar waveguides," *IEEE Photonics Technology Letters*, vol. 17, pp. 1884–1886, Sept. 2005.
- [32] M. Dai, L. Ma, Y. Xu, M. Lu, X. Liu, and Y. Chen, "Highly efficient and perfectly vertical chip-to-fiber dual-layer grating coupler," *Optics Express*, vol. 23, p. 1691, Jan. 2015.